

Magnetic signature of heavy metals pollution of sediments: case study from the East Lake in Wuhan, China

Tao Yang · Qingsheng Liu · Lungsang Chan ·
Zhendong Liu

Received: 6 August 2006 / Accepted: 5 December 2006 / Published online: 9 January 2007
© Springer-Verlag 2007

Abstract Detailed magnetic measurements and geochemical analyses were performed on 114 sediment samples collected from the East Lake, Wuhan city, China, to establish a possible link between the enhanced concentration of anthropogenic magnetic particles and heavy metals with known sources. Relatively higher magnetic susceptibility values (mass-specific, χ , $>150 \times 10^{-8} \text{ m}^3 \text{ kg}^{-1}$) were observed for samples near the pollution sources: e.g. the Wuhan Iron and Steel Company (WISC), the Qingshan Thermal Power Plant (QTPP), the banks (driveways) of the lake and near the sightseeing route of yachts on the lake. Moreover, χ is positively correlated to the concentration of Pb (correlation coefficient $r = 0.682$), but negatively or weakly correlated with both Zn and Cu. In contrast, anhysteretic remanent magnetization (ARM) is significantly correlated with these major heavy metals ($r = 0.645$ for Zn-ARM, 0.699 for Pb-ARM and 0.841 for Cu-ARM, respectively), which indicate that ARM

serves a better indicator for the pollution of heavy metals in this lake. Thermomagnetic analysis combined with magnetic hysteresis measurements revealed that magnetites in the pseudo-single-domain/multidomain grain-size regions are dominant. Scanning electron microscopy and energy dispersive X-ray examinations of the magnetic extracts showed that these Fe-rich particles have different morphologies: orange-peel structure, hollow structure with adhered smaller particles, Zr-rich melted-like irregular particles, pear-shaped spherules and spherules with slick surfaces. These features are typical for particles produced by anthropogenic activities. Because of the genetic relationship between the environmental setting of the East Lake and the nearby pollution sources, this study suggests that in situ magnetic surveys are sensitive to evaluate the environmental pollution on the lake bottom.

Keywords Magnetic susceptibility · Heavy metals · Pollution · Lake sediments · East Lake · Wuhan city

T. Yang · Q. Liu (✉)
Department of Geophysics,
China University of Geosciences,
Wuhan 430074, People's Republic of China
e-mail: lqs321@cug.edu.cn

L. Chan
Department of Earth Sciences,
The University of Hong Kong, Hong Kong,
People's Republic of China

Z. Liu
Institute of Geodesy and Geophysics,
Chinese Academy of Sciences, Wuhan 430077,
People's Republic of China

Introduction

Mineral magnetic measurements have been widely used for delineating the environmental pollution during the recent decades, because they are fast, cost-effective, non-destructive and sensitive (Thompson et al. 1980; Oldfield et al. 1985; Maher et al. 1999; Hanesch and Scholger 2002). The concept is based on the fact that many anthropogenic impacts on the environment (effluents from power plants, combustion of fossil fuel, metallurgical industries, smelters, traffic, wastewater, etc.) are accompanied by significant

emission of strongly magnetic particles (e.g. magnetite) bearing heavy metals (Petrovský et al. 2000; Knab et al. 2005). Identification of these particles in various ecosystems can contribute to locate pollution sources, to trace transport and distribution of pollutants and to reconstruct pollution history (Petrovský et al. 1998, 2000; Hanesch and Scholger 2002; Desenfant et al. 2004).

Lake sediments, as natural sinks, record the input of minerals and heavy metals of different origins from lithogenic/pedogenic as well as anthropogenic sources. They provide important information on dominant local contributions, such as geologic anomalies and/or pollution sources in their catchments (Jordanova et al. 2004). Anthropogenic sources of pollution in urban lakes basically comprise: (1) emissions from industrial and fossil fuel combustion processes (e.g. steel works and power generation); (2) particles from vehicles (e.g. exhaust particulates, brake lining dust, erosion of the bodyworks); (3) exotic materials (e.g. metallic fragments, slag, road surface and building materials); (4) fertilizers and pesticides (mostly transported from agricultural soils), sewage sludge, etc. Generally, the magnetic properties of the polluted sediments are mainly determined by the anthropogenic portion and to a smaller degree by the natural (lithologic/pedogenic) minerals (Jordanova et al. 2004).

Magnetic measurements have been employed recently by a number of authors in examining the anthropogenic inputs into lakes, as well as stream and marine sediments (Scholger 1998; Chan et al. 2001; Rose et al. 2004; Knab et al. 2005; Chaparro et al. 2005). Locke and Bertine (1986) used magnetite-bearing pollutants to describe the impact of coal burning history in recent lake, estuarine and marine sediments. Magnetic characteristics and concentrations of heavy metals were evaluated statistically in urban lake sediments by Charlesworth and Lees (1997) and in industrially loaded lake sediments and fluvisols by Georgeaud et al. (1997) and Petrovský et al. (1998, 2001). Investigations along the river Mur (Austria) showed a positive correlation between magnetic susceptibility and slag particles from iron production in river sediments, and a significant positive correlation of magnetic susceptibility to some heavy metals like Pb, Cu, Cr and Zn (Scholger 1998). Petrovský et al. (2000) discussed the effect of local pollution sources on the magnetic susceptibility of stream sediments from the Moldau River, Bohemia. A significant correlation between the magnetic susceptibility and the concentrations of Pb, Zn and Cu, as well as the Tomlinson pollution load index, were observed in seabed sedi-

ments of Penny's Bay, Hong Kong (Chan et al. 2001). Wehland et al. (2002) and Jordanova et al. (2004) reported results of detailed magnetic susceptibility screening and profiling of the Theiss and Danube River sediments in Romania and Bulgaria. Desenfant et al. (2004) tested the magnetic susceptibility of river sediments in terms of anthropogenic pollution in an area with negligible lithogenic contributions and reported the highest correlation between the concentration of magnetic particles and Pb as well as Zn in river sediments. A study of river sediments by Chaparro et al. (2003, 2004) proved that magnetic susceptibility is able to reflect industrial input into river sediments. Chaparro et al. (2005) found that the coercivity of remanence and the anhysteretic susceptibility/magnetic susceptibility-ratio correlate excellently with chemical variables in the lagoon and stream sediments from the Chascomus area (Argentina).

These correlations between magnetic parameters and heavy metal contents reveal a causal relation between iron oxides and heavy metals in sediments. This relationship could be based either on their joint genesis during the industrial process involved (e.g. incorporation of heavy metals into the lattice structure of ferrimagnetics during the combustion process), on joint transportation and deposition, or on adsorption of heavy metals on the surface of ferrimagnetic particles already present in the environment (Taylor et al. 1987; Cornell 1991; Rose and Bianchi-Mosquera 1993; Petrovský et al. 1998; Petrovský and Ellwood 1999). To a certain extent, the distribution of heavy metals in lake sediments is also constrained by the content of organic matter and the grain size of the sediment (Plater et al. 1998). The fine fraction of the sediments, with relatively large specific surfaces and rich in organic matter, may contain high levels of heavy metals and organic pollutants due to adsorption, deposition and ion exchange (Jain and Ram 1997; Huang and Lin 2003). Nevertheless, the common links between magnetic properties and pollutants demonstrate that mineral magnetic analysis can be applied successfully to delineate and recognize the sources and signatures of pollution in urban lake sediments.

In this study, emphasis is placed on the magnetic properties of the lake sediments and their association with heavy metal contents in sediments from the East Lake, the largest urban lake in China. The aim is to examine the magnetic properties of lake sediments, and to establish links between the enhanced concentrations of anthropogenic magnetic particles and heavy metals (e.g. Cu, Pb, Zn, etc.) with well-determined sources of pollution around the lake.

Environmental setting

The East Lake, the largest urban lake in China, lies northeast of Wuhan city and is close to (in downwind direction) Wuhan Iron and Steel Company (WISC) and Qingshan Thermal Power Plant (QTPP), a heavy industrial area (Fig. 1). A number of roadway dikes have been constructed across the lake, dividing it into several distinct water bodies. Inter-basin water exchange occurs only through bridge under-passes and culverts beneath the roadways. The water area and the average depth of the lake are respectively 27.9 km² and 3–4 m with a maximum depth of 4.75 m.

Urban expansion and industrial developments around the lake began in the 1950s. Since then, a large mass of atmospheric particles generated by industrial processes such as combustion of coal for power generation (e.g. QTPP), iron and steel production and non-ferrous metal smelting (e.g. WISC) must have been deposited in the lake. Sometimes, wastewater is released into the lake from the industrial areas. In addition, a large amount of wastewater has entered the lake from residential districts and hospitals through many small outlets, especially the southwest shore of the lake. With the rapid development of industrialization and urbanization, environmental pollution has been constantly increasing during the last decades.

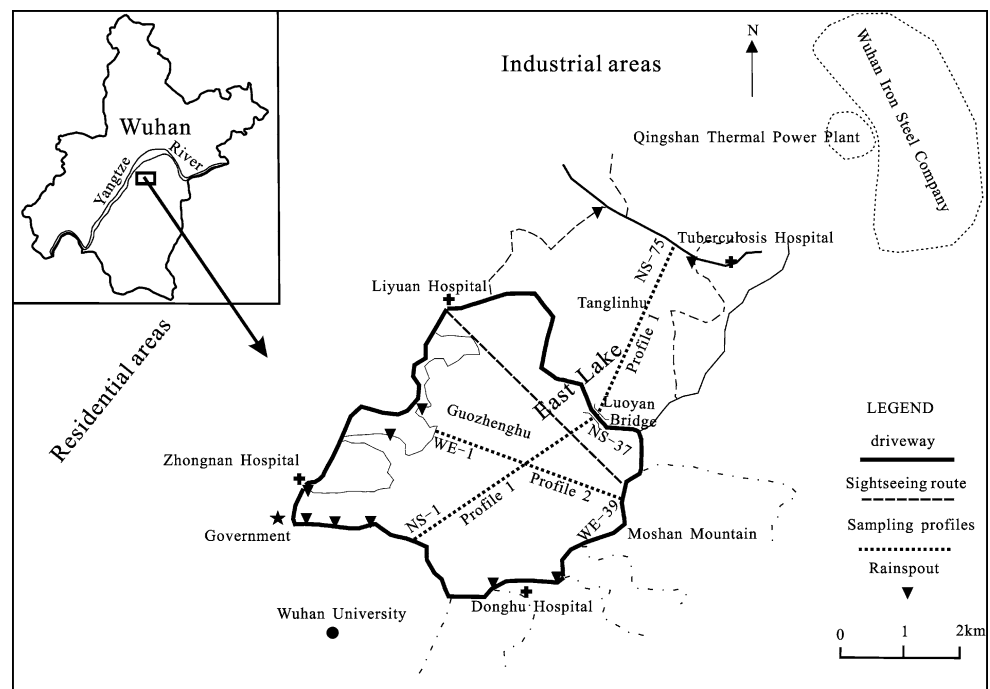
The sedimentation rate in the lake ranges from 2.1 to 7.8 mm a⁻¹ with an average of 4.6 mm a⁻¹. The basement of the lake is entirely sedimentary with sapropel, silty, sandy and clayey sediments, all with

extremely low magnetite content. This geological setting justifies the assumption that magnetic enhancement in the uppermost sediment samples can be attributed mostly to other sources than lithogenic. Therefore, atmospherically transported particles from WISC and QTPP are considered to be the most significant contribution of pollutants, because they are close to northeast of the study area, and the prevailing winds (northerly and northeast mistrals) allow for the southward and southwest-ward atmospheric transport of pollutants. In addition, the driveways along the shores and the sightseeing route from Moshan Park to East Lake Park on the lake may also contribute to the input of pollutants into the lake. Therefore, it is our observation that the magnetic signature of anthropogenic contributions should be well pronounced.

Sampling and methods

We collected 114 sediment samples along two crossed profiles (Fig. 1) and later these samples were dried at the room temperature. Magnetic susceptibility (χ , mass-specific) was measured using an AGICO KLY-3S Kappabridge. A vibrating sample model of the Princeton Micromag 2900 magnetometer was used to measure hysteresis loops with the maximum fields of 1.5 T. Hysteresis parameters, saturation magnetization (M_s), saturation remanence (M_{rs}) and coercive force (H_c) of 15 representative samples were obtained after subtracting the high-field slope, which is dominantly

Fig. 1 Location of the study area and the sampling profiles



controlled by paramagnetic minerals. To obtain the remanence coercivity (H_{cr}), after reaching 1 T, the samples were remagnetized using the backward field method. Following the diagram of Day et al. (1977), ratios of these parameters were used in magnetogranelometry. Anhysteretic remanent magnetization (ARM) was induced in a steady field of 0.05 mT imposed on a peak-alternating field of 100 mT. Low- and high-frequency (0.47 and 4.7 kHz) AC susceptibilities [χ_{lf} , χ_{hf} and $\chi_{fd}\%$ = $(\chi_{lf} - \chi_{hf})/\chi_{lf} \times 100\%$] were determined using a Bartington dual frequency magnetic susceptibility meter, MS2B. The analysis of magnetic phases of the selected samples was performed by measurements of the Curie temperature (T_c) using a KLY-3S Kappabridge equipped with a CS-3(L) furnace.

The total contents of chemical elements, such as Pb, Zn, Cu, Ni and Cr, etc. of the 30 samples were analysed by X-ray fluorescence using SRS303. The relative error of parallel samples was determined as less than 5%. Magnetic extracts of representative samples separated by using a hand magnet were observed under the environmental scanning electron microscope (ESEM) Quanta 200 after coating with carbon. The major element composition of selective grains was also measured using ESEM.

Results

χ and remanence

χ values of the two profiles (Fig. 2) show a gradual increase towards the banks of the lake, near the sightseeing route of yachts, and towards WISC and QTPP (Fig. 2a, d), where the χ is usually $>200 \times 10^{-8} \text{ m}^3 \text{ kg}^{-1}$ with a maximum value of $301.09 \times 10^{-8} \text{ m}^3 \text{ kg}^{-1}$ (Fig. 2a). For profile 2, χ is $>100 \times 10^{-8} \text{ m}^3 \text{ kg}^{-1}$ with a maximum value of $191.75 \times 10^{-8} \text{ m}^3 \text{ kg}^{-1}$ towards the banks. Magnetic parameters of the selected samples are summarized in Table 1. A significant negative correlation ($r = -0.648$) between χ and $\chi_{fd}\%$ is observed, which is one of the typical features of polluted materials. This strongly indicates that χ is controlled by coarse-grained magnetic particles. Otherwise, a positive correlation between them will hold, e.g. samples from the Chinese Loess Plateau (Liu et al. 2004). With increasing the concentration of the coarse-grained magnetic particles, the relative contribution of the fine-grained particles, which are responsible for $\chi_{fd}\%$, is decreased, resulting in a decrease in $\chi_{fd}\%$. Thus, the increase in χ generally reflects a gradual increase of the concentration of the coarse-grained magnetic minerals.

ARM, which is sensitive to fine-grained magnetic particles (e.g. SSD) ranges from 14.58 to $53.23 \times 10^{-5} \text{ A m}^2 \text{ kg}^{-1}$. Samples NS-13 and NS-32 have relatively low χ , ARM, M_s and M_{rs} , but high $\chi_{fd}\%$ ($>5\%$).

Magnetic hysteresis

All samples exhibit thin, ‘wasp-waisted’ hysteresis loops which are almost saturated at 300 mT (Fig. 3), indicative of the contribution of low coercivity ferromagnetic minerals (Roberts et al. 1995). Marked paramagnetic (Fig. 3b) and diamagnetic slopes (Fig. 3c) can be observed. H_c and H_{cr} range from 5.91 to 12.69 mT and 26.28 to 41.17 mT, respectively, indicating magnetite as the predominant magnetic phase. This finding is also supported by the plot of M_{rs} , χ and H_{cr} (Peters and Thompson 1998). All data form a close cluster within the (titano)magnetite area, probably slightly shifted towards the magnetically harder greigite area (Fig. 4).

Ratios of saturation remanence to saturation magnetization (M_{rs}/M_s) and coercivity of remanence to coercive force (H_{cr}/H_c) range between 0.06–0.16 and 2.85–5.11, respectively, which suggest magnetic particles within PSD and MD (pseudo-single-domain/multidomain) state (Day et al. 1977) (Fig. 5).

Temperature-dependent susceptibility (κ - T)

κ - T curves are widely used to identify ferromagnetic minerals. In general, there are two types of κ - T curves (Fig. 6). The heating curves show the presence of several ferrimagnetic phases or phase transformations. For example, there are phases with a lower T_c (320–350°C; inset in Fig. 6a) and a higher T_c of 580°C (magnetite). These phases have different relative contributions to the total signal in the samples, as observed from the different height of the high-temperature peak on the heating curves. Heating to temperatures above 500°C, there is a neoformation of a large amount of secondary magnetite, which is responsible for the large increase of κ for the cooling curves. Notably, the heating-induced κ values of samples NS-13 and NS-32 after cooling are about eight times higher than their initial values (Fig. 6a).

Heavy metal contents and their correlations with magnetic parameters

Concentrations of selected heavy metals in 30 representative sediment samples and their correlations with magnetic parameters are summarized in Table 2. The

Fig. 2 Comparison of magnetic susceptibility and heavy metal contents of the East Lake sediments

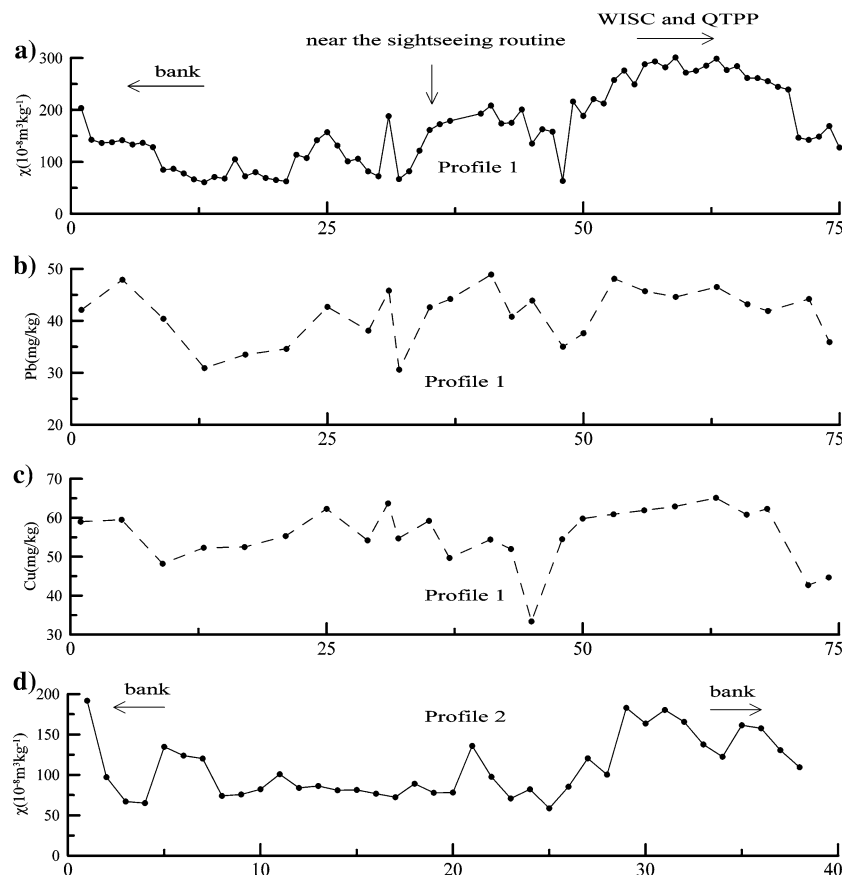


Table 1 Magnetic parameters of the selected samples

Samples	χ ($10^{-8} \text{ m}^3 \text{ kg}^{-1}$)	χ_{fd} (%)	ARM ($10^{-5} \text{ A m}^2 \text{ kg}^{-1}$)	H_c (mT)	H_{cr} (mT)	M_s ($10^{-3} \text{ A m}^2 \text{ kg}^{-1}$)	M_{rs} ($10^{-3} \text{ A m}^2 \text{ kg}^{-1}$)
NS-1	203.87	1.8	33.29	9.38	30.46	34.44	3.51
NS-5	141.80	3.3	46.68	10.64	31.30	24.90	3.01
NS-13	60.96	6.3	28.52	10.02	30.83	6.24	0.90
NS-25	157.25	2.6	47.65	9.13	27.66	24.64	2.61
NS-31	188.09	1.5	53.23	9.56	28.80	71.54	7.34
NS-32	67.00	5.2	19.55	10.89	31.43	17.69	2.87
NS-35	161.43	2.6	38.23	5.91	30.20	11.86	0.68
NS-37	179.11	1.1	23.92	7.10	30.16	6.43	0.47
NS-41	208.53	1.2	28.95	12.69	41.17	22.91	2.84
NS-45	135.22	1.0	14.58	8.13	28.31	12.43	0.92
NS-56	287.92	1.6	37.07	8.36	27.61	31.00	2.77
NS-63	298.65	1.3	42.65	7.56	28.57	39.91	3.46
NS-66	261.51	1.6	38.09	7.79	27.75	50.16	4.19
NS-68	255.58	2.2	35.43	9.05	29.48	43.14	4.14
NS-72	142.41	0.6	19.95	9.21	26.28	12.66	1.40
Max	298.65	6.3	53.23	12.69	41.17	71.54	7.34
Min	60.96	0.6	14.58	5.91	26.28	6.24	0.47
Mean	183.29	2.26	33.85	9.03	30.00	27.33	2.74
SD	71.74	1.60	11.27	1.68	3.44	18.19	1.78

contents of Cu, Zn and Pb are 1.5–1.8 times higher than those of background soils in the Wuhan region (China Environmental Monitoring Station 1990),

indicating that the lake has been polluted with Cu, Zn and Pb. This is considered to be the result of a gradual accumulation from various pollution sources over time,

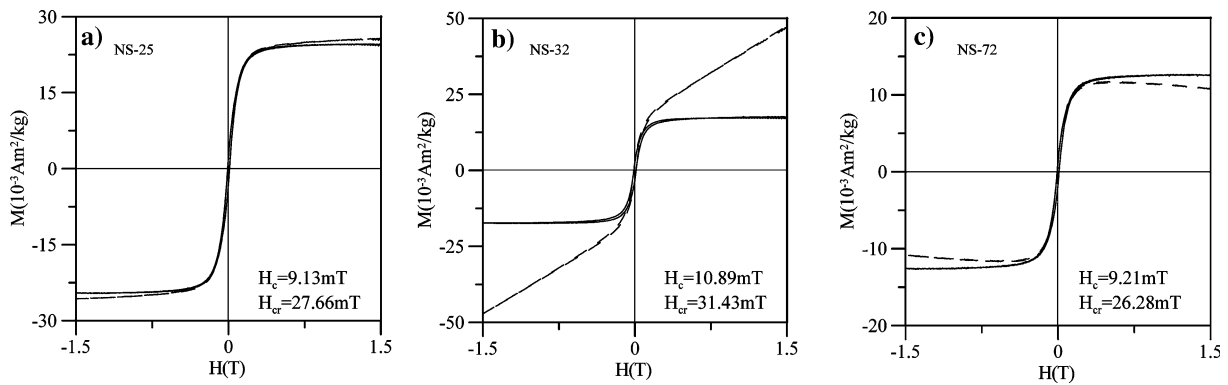


Fig. 3 Magnetic hysteresis loops for typical samples before (*dashed lines*) and after (*solid lines*) correction for the paramagnetic contributions

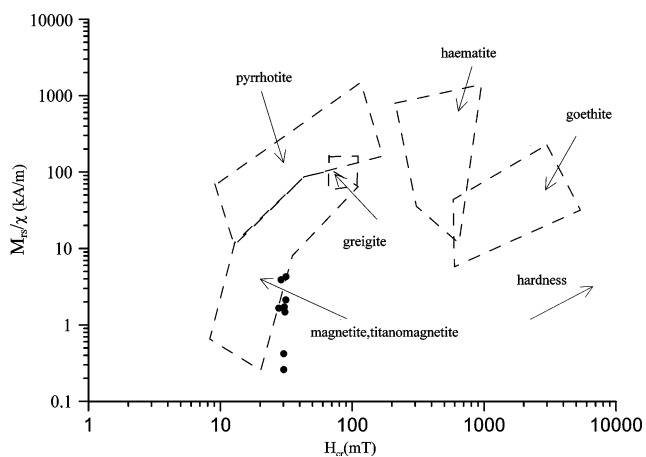


Fig. 4 Magnetic discrimination of minerals according to Peters and Thompson (1998). All samples form a compact cluster within the magnetite–titanomagnetite range

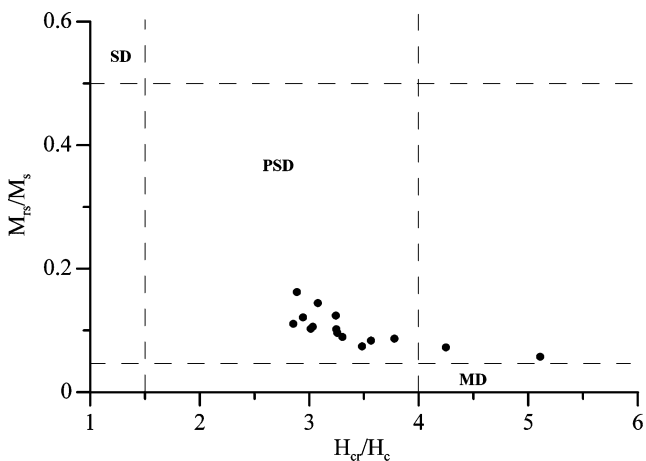


Fig. 5 Hysteresis ratios plotted on a Day diagram (Day et al. 1977). *SD*, single domain; *PSD*, pseudo-single domain; *MD*, multidomain

including industrial emissions, automobile exhausts and fly ashes.

Distributions of Pb and Cu in profile 1 are shown in Fig. 2b and c, respectively. High contents of Pb and Cu are present near the shores of the lake, especially adjacent to WISC and QTPP. The maximum content is 48.9 mg kg^{-1} for Pb and 65.1 mg kg^{-1} for Cu, 1.83 and 2.12 times higher than their corresponding background values.

Significant correlations are found between χ and the concentration of Pb; ARM and Zn, Pb, and Cu; M_s and Cu (Table 2). The correlation coefficients are 0.682 for Pb– χ , 0.841 for Cu–ARM, 0.645 for Zn–ARM and 0.745 for Cu– M_s (Fig. 7). The close correlation between χ and Pb can also be demonstrated by the good agreement of their variations along the profile (Fig. 2a, b). The correlation coefficients of heavy metal contents with ARM are higher than that with χ (Table 2).

Morphology and composition of magnetic particles

Scanning electron microscopy (SEM) revealed typical magnetic particles, mainly consisting of iron oxide(s). Similar spherules could be observed in most samples. Examples with different morphology and diameter are shown in Fig. 8. Energy dispersive X-ray (EDX) results show that both pure Fe-oxide particles and Fe-bearing compounds are present (Table 3). These particles have various morphologies: orange-peel structure, a hollow structure with adhered smaller particles, Zr-rich melted-like irregular particles (Zr is an important material for foundry, glass, ceramic and refractory industries), pear-shaped spherules and spherules with a slick surface.

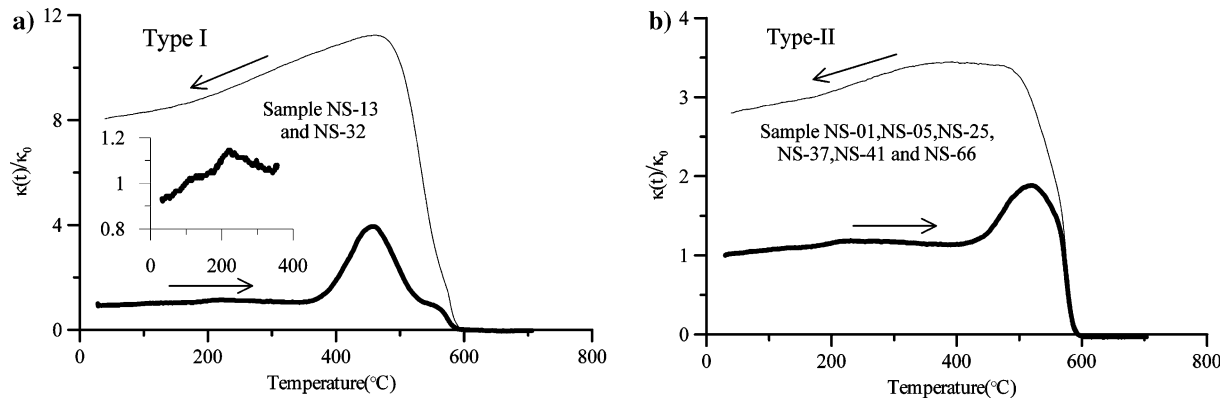


Fig. 6 Representative types of temperature dependence of magnetic susceptibility. The *inset* in (a) shows the heating curve of sample NS-13 between room temperature and 350°C

Table 2 Ranges, mean values and standard deviations (SD) of heavy metal contents (mg kg⁻¹), and coefficients of bi-variate correlation with selected magnetic parameters (*n* = 30)

	Zn	Pb	Cu
Range	104–177	30.6–48.9	33.4–65.1
Mean	138	40.3	54.8
SD	14.6	5.3	7.5
Background value ^a	83.6	26.7	30.7
Coefficients of bi-variate correlation			
χ	-0.284	0.682**	0.429*
ARM	0.645*	0.699**	0.841**
M_s	0.223	0.331	0.745**

*, ** Statistical significance at probability levels of <0.05 and <0.01, respectively

^a After China Environmental Monitoring Station (1990)

Discussion

Magnetic minerals in sediments

A poor correlation ($r = 0.414$) between M_{rs} and χ suggests that multiple magnetic mineral phases exist in the sediments (Peters and Dekkers 2003), which is also confirmed by κ - T curves (Fig. 6). The T_c of 580°C is typical for magnetite. The maximum κ between 400 and 580°C in the heating curve can be attributed to the Hopkinson peak and (or) to newly crystallized magnetite, perhaps due to alteration/decomposition of Fe-rich silicates/carbonates (e.g. clay-minerals) (Hoffmann et al. 1999; Chaparro et al. 2003), as indicated by the cooling curves with much higher κ values. Besides these pronounced features, another distinct phase transition between room temperature and 350°C is also presented in the heat run of samples type I (shown in inset in Fig. 6a). Between room temperature and 220°C, κ increases continuously and sharply decreases above that and reaches its lowest value at 320°C. It

subsequently increases again, which is typical for greigite (Roberts 1995; Torii et al. 1996). A similar phase was also found in the Moldau River sediments in south Bohemia (Petrovský et al. 2000). In addition, the increase of κ at 420°C could be due to the presence of a small amount of pyrite, which is transformed into magnetite (Emiroglu et al. 2004). However, these two transforms are much weaker than the phase transition at 580°C (magnetite), revealing that magnetite is the dominant magnetic carrier.

All hysteresis loops of the studied sediments are almost saturated at 300 mT (Fig. 3), suggesting that the predominant magnetic phase is a ferrimagnetic mineral with low coercivity. This shape of hysteresis loops is often observed in fly ashes produced by coal burning (Petrovský et al. 1998; Strzyszc and Magiera 2001). However, the ‘wasp-waisted’ shape indicates the presence of a small amount of high coercivity magnetic minerals (Roberts et al. 1995; Tauxe et al. 1996) that have been identified as iron sulphide phases (e.g. greigite and pyrite) by thermomagnetic analysis. The ‘soft’ behaviour of hysteresis loops (Fig. 3) as well as the low frequency dependence of magnetic susceptibility, which ranges from 0.6 to 3.3% (with two exceptions – NS-13 and NS-32; Table 1), are typical features that distinguish anthropogenic ferrimagnetics from natural ferrimagnetic minerals that occur often as superparamagnetic grains (Mullins 1977). This suggests that the magnetic properties of the studied sediments are controlled by anthropogenic ferromagnetic minerals (Magiera and Strzyszc 2000; Strzyszc and Magiera 2001).

Moreover, it is worth noting that the samples of type I (e.g. NS-13 and NS-32), with relatively lower χ (77.96×10^{-8} and 76.57×10^{-8} m³ kg⁻¹, respectively), but higher $\chi_{fd}\%$ (>5%, Table 1), show different behaviour between room temperature and 320°C in the

Fig. 7 Scatter plots of mass-specific susceptibility, M_s and ARM versus Cu, Pb and Zn

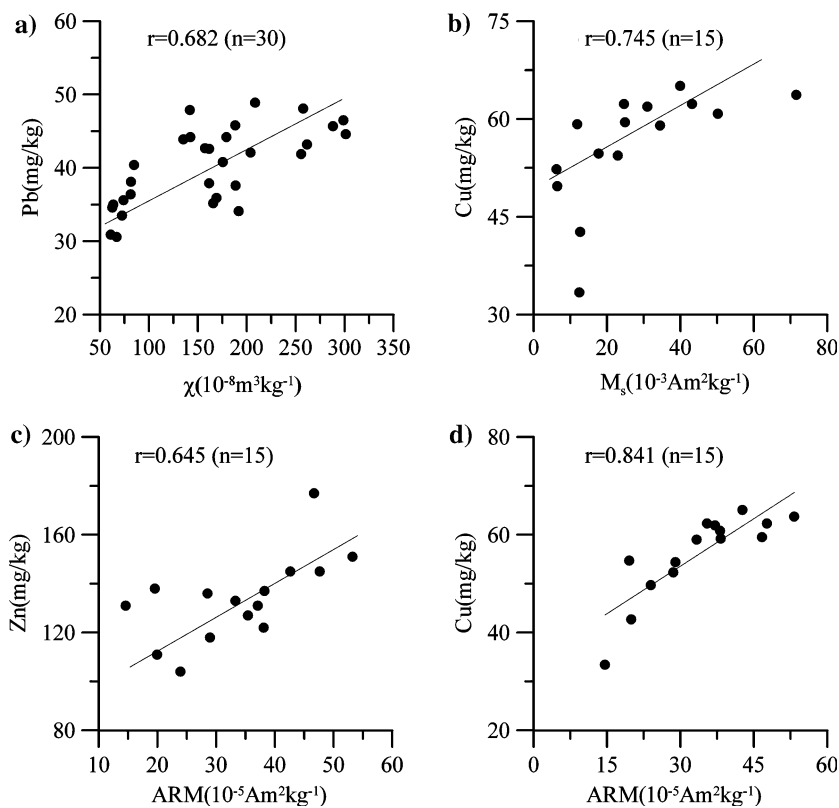
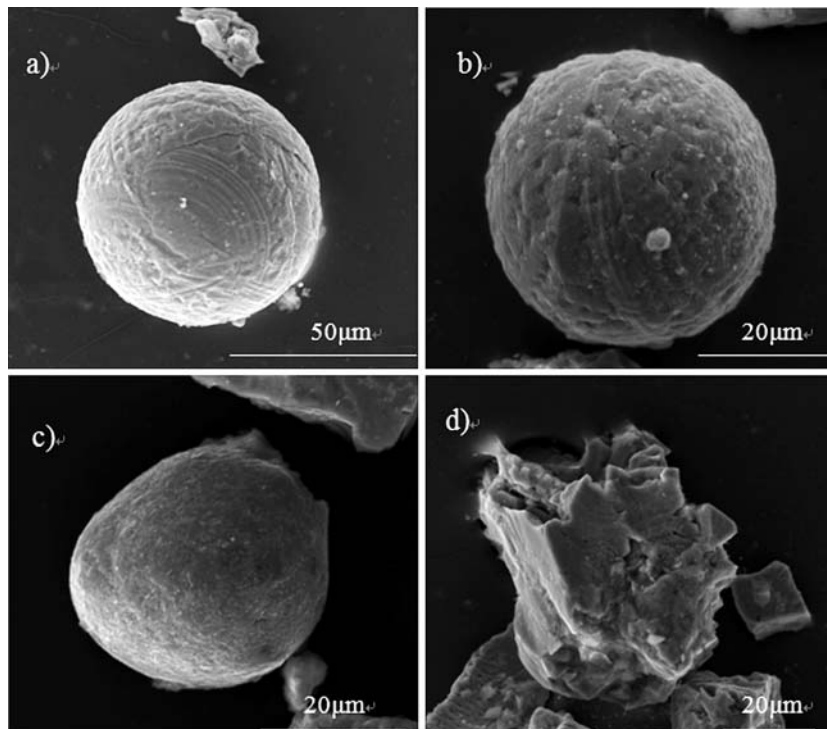


Fig. 8 Representative SEM micrographs of magnetic particles. **a** Only iron oxide identified, $d \approx 60 \mu\text{m}$; **b** strongly magnetic Fe-spherule with ‘orange-peel’ structure and adhered smaller particles on the surface, $d \approx 43 \mu\text{m}$; **c** pear-shaped spherule containing Cd, $d \approx 40 \mu\text{m}$; **d** Zr-rich melted-like irregular particle



κ - T curves (Fig. 6a). Their hysteresis loops also show a much higher paramagnetic component (Fig. 3b). These characteristics may be due to the presence of a small

amount of fine-grained iron sulphide (e.g. greigite), which may be formed authigenically in anoxic sedimentary environments (Roberts and Weaver 2005).

Table 3 Composition of representative magnetic particles in Fig. 8 (unit, wt%)

Particles	O	Fe	Mg	Al	Si	Cl	K	Ca	Cd	Zr
a	22.53	77.47								
b	24.15	74.85		0.33	0.38	0.29				
c	40.93	27.04		12.19	19.74				0.10	
d	33.23	43.87	2.79	0.88	0.39	0.29	0.04	0.30		18.21

However, Roberts and Weaver (2005) suggested that greigite is a problematical mineral for environmental magnetism and paleomagnetism, and its presence should be a cause for concern in studies that require interpretation of syndepositional geophysical, geochemical or geological signals. Therefore, the details may need further studies in future.

Source of magnetic particles and heavy metals

The origin of the magnetic fraction in the anthropogenic pollution is connected with high-temperature processes during producing and processing materials with significant Fe content. One of the dominant sources of such pollution is power plants and metallurgical, metal-processing and smelting industries. The coals used in power plants usually contain a significant portion of Fe-bearing minerals like pyrite, markasite and/or siderite. During coal combustion, these minerals transform in different ways, but the final result is a magnetite-like phase occurring as single spherule-like grains (Jordanova et al. 2004). The metal-processing industry, which is also connected with high-temperature burning processes in the blast furnaces, is another major source of environmental pollution. During the high-temperature processes, magnetic spherical particles are usually formed (McLennan et al. 2000; Sokol et al. 2002). In addition to these combustion-related particles, non-spherical magnetite particles can be generated by vehicles, via exhaust emissions and abrasion/corrosion of engine and/or vehicle body material (Olson and Skogerboe 1975).

Theis and Wirth (1977) suggested that most of the heavy metals in fly ashes emitted by coal combustion are related to iron, manganese and aluminous oxides: Cu, Cr, As and Zn always accompany iron oxide(s); Cr and Ni mainly exist in manganese oxide and Pb is present in both iron and manganese oxide(s). Hullet et al. (1980) found that certain transition metals, such as V, Cr, Mn, Co, Ni, Zn and Cu in the fly ashes of power plants, are associated with magnetic minerals and are mostly present in the form of substituted spinels. Also, the magnetic fraction in smelting slags is usually represented by magnetite, sulphides and metallic phases. Depending on the efficiency of pyrometallurgical and metal recovery processes, smelting

slags can be enriched in metals (e.g. Pb, Cu and Zn) to different degrees (Lottermoser 2002). Therefore, a strong correlation of these metals with magnetic parameters is expected, which is also one of the indispensable conditions for mapping environmental pollution using magnetic measurements.

The prevailing wind direction is north and northeast in Wuhan city, while the East Lake is located in the downwind area (Fig. 1). Driven by the wind, fly ashes and other aerosols bearing heavy metals produced by both WISC and QTPP are deposited into the lake. These spherules (Fig. 8), rich in iron oxide(s), are characteristic for particles derived from combustion processes (Maher et al. 1999; Petrovský et al. 1998, 2000). Similar composition and morphology of the fly ashes particles were reported in a number of studies (Hanesch and Scholger 2002; Kukier et al. 2003; Desenfant et al. 2004; Knab et al. 2005). Thus, it is inferred that the emissions from WISC and QTPP are the predominant cause accounting for the increasing concentrations of magnetic minerals and heavy metals in lake sediments.

The increased concentrations of magnetic minerals near the shores and driveways may result from rain-washing of paving materials, abrasion of tyres and emissions of vehicles, which often contain PSD/MD magnetite-like particles bearing significant contents of Cu, Pb and Zn (Hoffmann et al. 1999; Petrovský et al. 2000; Kapička et al. 2003; Lu et al. 2005); yacht-related contamination caused by emissions from fuel burning, servicing, scraping and re-painting may be the reason for higher magnetic parameters and heavy metals near the sightseeing route. Similar activities cause increasing susceptibility in the seabed sediments of Penny’s Bay, Hong Kong, as reported by Chan et al. (2001). In East Lake area, the atmospheric particles are mainly derived from industrial processes such as combustion of coal for power generation (e.g. QTPP), iron and steel manufacture and non-ferrous metal smelting (e.g. WISC) (compare profile 1, Fig. 2).

Magnetic parameters as indicators of heavy metal contaminations

Generally, two conditions must be met to use magnetic measurements as a measure of heavy metals contami-

nation: (1) χ must be greater than the background level; (2) the magnetic parameters display a significant correlation with the concentration of heavy metals (Versteeg et al. 1995). The present study showed that the urban lake sediments satisfy both conditions. χ near shores and the sightseeing route of yachts on the lake is $>150 \times 10^{-8} \text{ m}^3 \text{ kg}^{-1}$ with a maximum of $203.87 \times 10^{-8} \text{ m}^3 \text{ kg}^{-1}$. Towards WISC and QTPP, it is higher than $200 \times 10^{-8} \text{ m}^3 \text{ kg}^{-1}$ with a maximum value of $301.09 \times 10^{-8} \text{ m}^3 \text{ kg}^{-1}$, which is much higher than that of the samples from the centre of the lake (Fig. 2). Although spatially higher χ values are consistent with the distribution of the pollution sources, they are only weakly correlated with heavy metals (except for Pb). In contrast, ARM significantly correlates with Pb, Cu and Zn, with correlation coefficients of 0.699, 0.841 and 0.645, respectively, demonstrating that remanent magnetic parameters are better indicators for pollution by heavy metals in this lake. Similar results were reported in other studies. Georgeaud et al. (1997) found that the contents of heavy metals correlated better with SIRM than with χ . Chaparro et al. (2003) also found a better correlation between ARM and heavy metals than between χ and heavy metals.

The weak correlation between χ and heavy metal contents may be due to the presence of different magnetic minerals, to different concentrations of heavy metals in complex sources and to various physical and chemical changes occurring both during their transport to the lake and after deposition. A strong correlation between χ and heavy metals only exists for polluted samples of enhanced χ , like those that carry magnetic inclusions (Schmidt et al. 2005). Similar results were reported by Beckwith et al. (1986), who found that the correlation between heavy metals and χ is lost if sediment samples with low χ were added to the statistical analysis. Charlesworth and Lees (1997) found that there appears to be no relationship between heavy metals and mineral magnetic properties in urban lake (Swanswell Pool) sediments in Coventry. Schmidt et al. (2005) suggested that the best correlation of results is obtained using samples of χ higher than a site-specific threshold. Another possible cause for low correlations is the effect of dissolution/transformation of magnetic particles resulting in a decrease of magnetic concentration in aqueous environments (Petrovský et al. 1998; Emiroglu et al. 2004), as for example in a lake whose water was acidified due to a nearby power plant (Hu et al. 2003). Therefore, in this kind of magnetic investigation of industrial pollution, a thorough investigation both of individual pollution sources and the sedimentary environment should be done, which is a challenge to our further studies.

Conclusions

Detailed magnetic measurements and geochemical analyses were performed on sediments from the East Lake, Wuhan city. Magnetic susceptibility, which has been used in other studies as an indicator of pollution levels, exhibits elevated values (usually $>150 \times 10^{-8} \text{ m}^3 \text{ kg}^{-1}$ with a maximum of $301.09 \times 10^{-8} \text{ m}^3 \text{ kg}^{-1}$) towards the shores (driveways) of the lake, in proximity to WISC and QTPP, and near the sightseeing route of yachts. Magnetic susceptibility is the lowest in the centre of the lake. Only the concentration of Pb is closely correlated to susceptibility (with a correlation coefficient of 0.682), in contrast to Zn and Cu. ARM, however closely correlates with Zn, Pb and Cu, the correlation coefficients being 0.645, 0.699 and 0.841, respectively. These results suggest that ARM is a better indicator for pollution in the studied lake. Thermomagnetic analysis combined with magnetic hysteresis measurements on the selected samples suggested that a PSD/MD magnetite-like phase dominates the magnetic phases in the sediments. SEM/EDX examination of the magnetic extracts revealed that these particles are rich in iron oxides and have various morphologies: orange-peel structure, hollow structure with adhered smaller particles, Zr-rich melted-like irregular particles, pear-shaped spherules and spherules with a slick surface. Combined with the environmental settings of the lake, it is inferred that these magnetic particles are derived from anthropogenic activities, such as combustion, steel processing, metal smelting, abrasion of tyres, emissions of vehicles, pavement materials, and so on. Accordingly, the WISC and QTPP, vehicles on roads along the lakeshore and yachts on the lake can be considered as major pollution sources. These results make it possible to use magnetic techniques as simple, rapid and non-destructive tools for assessing the heavy metal pollutions in the investigated lake.

Acknowledgments This study was supported by the National Natural Science Foundation of China (No. 40474025). We thank Dr Q.S. Liu for improving the language and the anonymous reviewers for their helpful comments.

References

- Beckwith PR, Ellis JB, Revitt DM, Oldfield F (1986) Heavy metals and magnetic relationships for urban source sediments. *Phys Earth Planet Inter* 42:67–75
- Chan LS, Ng SL, Davis AM, Yim WWS, Yeung CH (2001) Magnetic properties and heavy-metal contents of contaminated seabed sediments of Penny's bay, Hong Kong. *Mar Pollut Bull* 42:569–583

- Chaparro MAE, Bidegain JC, Sinito AM, Gogorza CSG, Jurado S (2003) Preliminary results of magnetic measurements on stream-sediments from Buenos Aires Province, Argentina. *Stud Geophys Geod* 47:121–145
- Chaparro MAE, Bidegain JC, Sinito AM, Jurado SS, Gogorza CSG (2004) Magnetic studies applied to different environments (soils and stream sediments) from a relatively polluted area in Buenos Aires Province, Argentina. *Environ Geol* 45:654–664
- Chaparro MAE, Lirio JM, Nunez H, Gogorza CSG, Sinito AM (2005) Preliminary magnetic studies of lagoon and stream sediments from Chascomus area (Argentina)—magnetic parameters as indicators of heavy metal pollution and some results of using an experimental method to separate magnetic phases. *Environ Geol* 49:30–43
- Charlesworth SM, Lees JA (1997) The use of mineral magnetic measurements in polluted urban lakes and deposited dusts, Coventry, U.K. *Phys Chem Earth* 22(1–2):203–206
- China Environmental Monitoring Station (1990) Background values of elements in soils of China. China Environmental Press, Beijing (in Chinese)
- Cornell RM (1991) Simultaneous incorporation of Mn, Ni and Co in the goethite (α -FeOOH) structure. *Clay Miner* 26:427–430
- Day R, Fuller M, Schmidt V (1977) Hysteresis properties of titanomagnetites: grain-size and compositional dependence. *Phys Earth Planet Inter* 13:260–267
- Desenfant F, Petrovský E, Rochette P (2004) Magnetic signature of industrial pollution of stream sediments and correlation with heavy metals: case study from South France. *Water Air Soil Pollut* 152:297–312
- Emiroglu S, Rey D, Petersen N (2004) Magnetic properties of sediment in the Ria de Arousa (Spain): dissolution of iron oxides and formation of iron sulphides. *Phys Chem Earth* 29:947–959
- Georgeaud VM, Rochette P, Ambrosi JP, Vandamme D, Williamson D (1997) Relationship between heavy metals and magnetic properties in a large polluted catchment: the Etang de Berre (South of France). *Phys Chem Earth A* 22:211–214
- Hanesch M, Scholger R (2002) Mapping of heavy metal loadings in soils by means of magnetic susceptibility measurements. *Environ Geol* 42:857–870
- Hoffmann V, Knab M, Appel E (1999) Magnetic susceptibility mapping of roadside pollution. *J Geochem Explor* 66:313–326
- Hu S, Wang Y, Appel E, Zhu Y, Hoffmann V, Shi C, Yu Y (2003) Magnetic responses to acidification in Lake Yangzonghai, SW China. *Phys Chem Earth* 28:711–717
- Huang KM, Lin S (2003) Consequences and implication of heavy metal spatial variations in sediments of the Keelung River drainage basin, Taiwan. *Chemosphere* 53:1113–1121
- Hullet LD, Weinberger AJ, Northcutt KJ, Ferguson M (1980) Chemical species in fly ash from coal-burning power plant. *Science* 210:1356–1358
- Jain CK, Ram D (1997) Adsorption of lead and zinc on bed sediments of the river Kali. *Water Res* 31(1):154–162
- Jordanova D, Hoffmann V, Fehr KT (2004) Mineral magnetic characterization of anthropogenic magnetic phases in the Danube river sediments (Bulgarian part). *Earth Planet Sci Lett* 221:71–89
- Kapička A, Jordanova N, Petrovský E, Podrazský X (2003) Magnetic study of weakly contaminated forest soils. *Water Air Soil Poll* 148:31–44
- Knab M, Hoffmann V, Petrovský E, Kapička A, Jordanova N, Appel E (2005) Surveying the anthropogenic impact of the Moldau river sediments and nearby soils using magnetic susceptibility. *Environ Geol*. doi: 10.1007/s00254-005-0080-5
- Kukier U, Fauziah Ishak C, Summer ME, Miller WP (2003) Composition and element solubility of magnetic and non-magnetic fly ash fractions. *Environ Pollut* 123:255–266
- Liu QS, Banerjee SK, Jackson MJ, Maher BA, Deng CL, Pan YX, Zhu RX (2004) Mechanism of the magnetic susceptibility enhancements of the Chinese loess. *J Geophys Res* 109:B12107. doi:10.1029/2004JB003249
- Locke G, Bertine KK (1986) Magnetic sediments as an indicator of coal combustion. *Appl Geochem* 1:345–356
- Lottermoser BG (2002) Mobilization of heavy metals from historical smelting slag dumps, North Queensland, Australia. *Miner Mag* 66:475–490
- Lu SG, Bai SQ, Cai JB, Xu C (2005) Magnetic properties and heavy metal contents of automobile emission particulates. *J Zhejiang Univ Sci* 6B(8):731–735
- Magiera T, Strzyszczyk Z (2000) Ferrimagnetic minerals of anthropogenic origin in soils of some Polish national parks. *Water Air Soil Pollut* 124:37–48
- Maher BA, Thompson R, Hounslow MW (1999) Introduction. In: Maher BA, Thompson R (eds) Quaternary climates, environments and magnetism. Cambridge University Press, Cambridge, pp 1–48
- McLennan AR, Bryant GW, Stanmore BR, Wall TF (2000) Ash formation mechanism during combustion in reducing conditions. *Energy Fuels* 14:150–159
- Mullins CE (1977) Magnetic susceptibility of the soil and its significance in soil science—a review. *J Soil Sci* 28:223–246
- Oldfield F, Hunt A, Jones MDH, Chester R, Dearing JA, Olsson L, Prospero JM (1985) Magnetic differentiation of atmospheric dusts. *Nature* 317:516–518
- Olson KW, Skogerboe RK (1975) Identification of soil lead compounds from automotive sources. *Environ Sci Technol* 9:227–230
- Peters C, Dekkers MJ (2003) Selected room temperature magnetic parameters as a function of mineralogy, concentration and grain size. *Phys Chem Earth* 28:659–667
- Peters C, Thompson R (1998) Magnetic identification of selected natural iron oxides and sulphides. *J Magn Magn Mater* 183:365–374
- Petrovský E, Ellwood B (1999) Magnetic monitoring of air, land and water pollution. In: Maher BA, Thompson R (eds) Quaternary climates, environments and magnetism. Cambridge University Press, Cambridge, pp 279–322
- Petrovský E, Kapička A, Zapletal K, Sebestova E, Spanila T, Dekkers MJ, Rochette P (1998) Correlation between magnetic parameters and chemical composition of lake sediments from Northern Bohemia—preliminary study. *Phys Chem Earth* 23(9–10):1123–1126
- Petrovský E, Kapička A, Jordanova N, Knab M, Hoffmann V (2000) Low-field magnetic susceptibility: a proxy method of estimating increased pollution of different environmental systems. *Environ Geol* 39:312–318
- Petrovský E, Kapička A, Jordanova N, Boruvka L (2001) Magnetic properties of alluvial soils contaminated with lead, zinc and cadmium. *J Appl Geophys* 48:127–136
- Plater AJ, Ridgway J, Appleby PG, Berry A, Wright MR (1998) Historical contaminant fluxes in the Tees Estuary, UK: geochemical, magnetic and radionuclide evidence. *Mar Pollut Bull* 37:343–360
- Roberts AP (1995) Magnetic properties of sedimentary greigite (Fe_3S_4). *Earth Planet Sci Lett* 134:227–236
- Roberts AP, Weaver R (2005) Multiple mechanisms of remagnetization involving sedimentary greigite (Fe_3S_4). *Earth Planet Sci Lett* 231:263–277

- Roberts AP, Cui Y, Verosub KL (1995) Wasp-waisted hysteresis loops: mineral magnetic characteristics and discrimination of components in mixed magnetic systems. *J Geophys Res* 100(B9):17909–17924
- Rose AW, Bianchi-Mosquera GC (1993) Adsorption of Cu, Pb, Zn, Co, Ni and Ag on goethite and hematite: a control on metal mobilization from red beds into stratiform copper deposits. *Econ Geol* 88:1226–1236
- Rose NL, Boyle JF, Du Y, Yi C, Dai X, Appleby PG, Bennion H, Cai S, Yu L (2004) Sedimentary evidence for changes in the pollution status of Taihu in the Jiangsu region of eastern China. *J Paleolimnol* 32:41–51
- Schmidt A, Yarnold R, Hill M, Ashmore M (2005) Magnetic susceptibility as proxy for heavy metal pollution: a site study. *J Geochem Explor* 85:109–117
- Scholger R (1998) Heavy metal pollution monitoring by magnetic susceptibility measurements applied to sediments of the river Mur (Styria, Austria). *Eur J Environ Eng Geophys* 3:25–37
- Sokol EV, Kalugin V, Nigmatulina E, Volkova N, Frenkel A, Maksimova N (2002) Ferrospheres from fly ashes of Chelyabinsk coals: chemical composition, morphology and formation conditions. *Fuel* 81:867–876
- Strzyszczyk Z, Magiera T (2001) Record of industrial pollution in Polish ombrotrophic peat bogs. *Phys Chem Earth A* 26(11–12):859–866
- Tauxe L, Mullender TAT, Pick T (1996) Potbellies, wasp-waists, and superparamagnetism in magnetic hysteresis. *J Geophys Res* 101:571–583
- Taylor RM, Maher BA, Self PG (1987) Magnetite in soils. I. The synthesis of superparamagnetic and single domain magnetite. *Clay Miner* 22:411–422
- Theis TL, Wirth JL (1977) Sorptive behavior of trace metals on fly ash in aqueous systems. *Environ Sci Technol* 11:1096–1100
- Thompson R, Bloemendal J, Dearing JA, Oldfield F, Rummary TA, Stober JC, Turner GM (1980) Environmental applications of magnetic measurements. *Science* 207:481–486
- Torii M, Fukuma K, Horng CS, Lee TQ (1996) Magnetic discrimination of pyrrhotite and greigite bearing sediment samples. *Geophys Res Lett* 23(14):1813–1816
- Versteeg JK, Morris WA, Rukavina NA (1995) The utility of magnetic properties as a proxy for mapping contamination in Hamilton Harbor sediments. *J Great Lakes Res* 21:71–83
- Wehland F, Panaiotu C, Appel E, Hoffmann V, Jordanova D, Jordanova N, Denut I (2002) The dam breakage of Baia Mare—a pilot study of magnetic screening. *Phys Chem Earth* 27:1371–1376